

Charmed meson production pattern in PbPb collisions at the LHC

I.P. Lokhtin,^{1,*} A.V. Belyaev,¹ G.Kh. Eyyubova,¹ G. Ponimatkin,² and E.Yu. Pronina¹

¹ *Skobeltsyn Institute of Nuclear Physics, Moscow State University, RU-119991 Moscow, Russia*

² *Ostrov Industrial High School, Ostrov, Karlovy Vary District, Czech Republic*

The phenomenological analysis of various characteristics of J/ψ and D mesons in PbPb collisions at the center-of-mass energy 2.76 TeV per nucleon pair is presented. The data on charmed meson momentum spectra and elliptic flow are reproduced by two-component model HYDJET++ including thermal and non-thermal production mechanisms. The significant part of D -mesons is found to be in a kinetic equilibrium with the created medium, while J/ψ -mesons are characterized by earlier (as compared to light hadrons) freeze-out.

PACS numbers: 25.75.Ld, 24.10.Nz, 25.75.Bh

I. INTRODUCTION

Heavy quarks are predominantly produced in hard scatterings on a short time-scale and traverse the surrounding medium interacting with its constituents. Thus the production of hadrons containing heavy quark(s) is a particularly useful tool to probe transport properties of hot matter formed in ultrarelativistic heavy ion collisions. The modern pattern of multi-particle production in central heavy ion collisions at RHIC and LHC energies supposes the formation of hot strongly-interacting matter with hydrodynamical properties (“quark-gluon fluid”), which absorbs energetic quarks and gluons due to their multiple scattering and medium-induced energy loss (see, e.g., [1–5]). Within such paradigm, a number of questions related to heavy flavor production is definitely of interest. Are heavy quarks thermalized in quark-gluon plasma? Are charmed hadrons in a kinetic equilibrium with the created medium? What is the interplay between thermal and non-thermal mechanisms of hidden and open charm production?

The interesting measurements at the LHC involving momentum and centrality dependencies of charmed meson production and its azimuthal anisotropy in PbPb collisions at center-of-mass energy 2.76 TeV per nucleon pair have been done by ALICE [6–17] ATLAS [18] and CMS [19, 20] Collaborations. At that a number of theoretical calculations and Monte-Carlo simulations in different approaches were attempted to reproduce these data [21–31]. Note that the simultaneous description of momentum spectra (nuclear modification factors) and elliptic flow coefficients of charmed mesons is currently the challenging problem for most theoretical models. In this paper, the LHC PbPb data on momentum spectra and elliptic flow of charmed hadrons (D^\pm , $D^{*\pm}$, D^0 and J/ψ mesons) are analyzed and interpreted within two-component HYDJET++ model [32]. Among other heavy ion event generators, HYDJET++ focuses on the simulation of jet quenching effect taking into account

medium-induced radiative and collisional partonic energy loss (hard “non-thermal” component), and reproducing the main features of nuclear collective dynamics by the parametrization of relativistic hydrodynamics with preset freeze-out conditions (soft “thermal” component). It has been shown in the previous papers [33–36] that the model is able to reproduce the experimental LHC data on various physical observables measured in PbPb collisions, such as centrality and pseudorapidity dependence of inclusive charged particle multiplicity, transverse momentum spectra of inclusive and identified (π , K , p) hadrons, $\pi^\pm\pi^\pm$ femtoscopic correlation radii, momentum and centrality dependencies of elliptic and higher-order harmonic coefficients, dihadron angular correlations and event-by-event fluctuations of anisotropic flow. The next step is to apply this model for phenomenological analysis of LHC data on charmed hadron production.

II. SIMULATION OF CHARM PRODUCTION IN HYDJET++ MODEL

HYDJET++ is the model of relativistic heavy ion collisions, which includes two independent components: the soft hydro-type state (“thermal” component) and the hard state resulting from the medium-modified multi-parton fragmentation (“non-thermal” component). When the Monte-Carlo generation of both components in each heavy ion collision is completed, the overall final particle spectrum is formed by natural way as the junction of these two independent event outputs. The details of the model and corresponding simulation procedure can be found in the HYDJET++ manual [32]. Main features of the model are listed below as follows.

A. Soft component

The soft component represents the hadronic state generated on the chemical and thermal freeze-out hypersurfaces obtained from the parametrization of relativistic hydrodynamics with preset freeze-out conditions (the adapted event generator FAST MC [37, 38]). It is

*Electronic address: Igor.Lokhtin@cern.ch

supposed that a hydrodynamic expansion of the fireball ends by a sudden system breakup (“freeze-out”) at given temperature T . Thermal production of charmed hadrons is treated within the statistical hadronization approach [39, 40]. The momentum spectrum of the produced charmed hadrons retains the thermal character of the (partially) equilibrated Lorentz invariant distribution function in the fluid element rest frame:

$$f_c(p^{*0}; T, \gamma_c) = \frac{\gamma_c^{n_c} g_i}{\exp(p^{*0}/T) \pm 1}, \quad (1)$$

where p^{*0} is the hadron energy in the fluid element rest frame, $g_i = 2J_i + 1$ is the spin degeneracy factor, $\gamma_c \geq 1$ is the charm enhancement factor (or charm fugacity), and n_c is the number of charm quarks and antiquarks in a hadron C ($C = D, J/\psi, \Lambda_c$). The signs \pm in the denominator account for the quantum statistics of a fermion or a boson, respectively. The fugacity γ_c takes into account the enhanced yield of charmed hadrons as compared with its thermal number. Let us mark that the recombination of $c\bar{c}$ pairs to J/ψ -mesons during the hadronization stage is effectively taken into account within such an approach. The fugacity can be treated as a free parameter of the model, or calculated through the number of charm quark pairs obtained from perturbative QCD and multiplied by the number of nucleon-nucleon sub-collisions.

The mean charmed hadron multiplicities \overline{N}_c are determined through the corresponding thermal numbers using the effective volume approximation:

$$\overline{N}_c = \rho_c^{\text{eq}}(T) V_{\text{eff}}, \quad \rho_c^{\text{eq}}(T) = \int d^3p^* f_c(p^{*0}; T, \gamma_c), \quad (2)$$

where $\rho_c^{\text{eq}}(T)$ is the thermal (equilibrium) density of hadrons of type C at the temperature T , and V_{eff} is the total effective volume of hadron emission from the hypersurface of proper time $\tau = \text{const}$. The latter is calculated at given impact parameter b of a heavy ion collision as

$$V_{\text{eff}} = \tau \int_0^{2\pi} d\phi \int_0^{R(b, \phi)} \sqrt{1 + \delta(b) \tanh^2 Y_T(r, b) \cos 2\phi} \cosh Y_T(r, b) r dr \int_{\eta_{\min}}^{\eta_{\max}} Y_L(\eta) d\eta, \quad (3)$$

where $Y_L(\eta)$ and $Y_T(r, b)$ are longitudinal (Gaussian) and transverse (linear) flow rapidity profiles respectively, $R(b, \phi)$ is the fireball transverse radius in the azimuthal direction ϕ , and $\delta(b)$ is the momentum anisotropy parameter (the hydro-inspired parametrization [41] is implemented in HYDJET++ for the momentum and spatial anisotropy of a thermal hadron emission source). Since V_{eff} is a functional of the field of collective velocities on the freeze-out hypersurface, in fact the hadron spectrum is constructed as the superposition of thermal distribution and collective flow. The simulation procedure includes generation of a hadron four-momentum in the liq-

uid element rest frame in accordance with the equilibrium distribution function, generation of a spatial position and local four-velocity of the liquid element in accordance with the phase space and the character of fluid motion, boost of the hadron four-momentum in the event center-of-mass frame, and finally two- and three-body decays of resonances with branching ratios taken from the SHARE particle decay table [42]. At first the value V_{eff} is calculated for central collisions ($b = 0$), and then for non-central collisions it is supposed to be proportional to the mean number of nucleons-participants at given b . The event-by-event simulation of hadron production assumes the Poisson multiplicity distribution around its mean value for each hadron species.

The scenario with different chemical and thermal freeze-outs is implemented in HYDJET++. It means that particle number ratios are fixed at chemical freeze-out temperature T^{ch} , while the effective thermal volume V_{eff} and hadron momentum spectra being computed at thermal freeze-out temperature $T^{\text{th}} \leq T^{\text{ch}}$. Introducing the temperature of chemical freeze-out (lower than hadronization temperature T_c) and the temperature of thermal freeze-out effectively trace the stages of inelastic (between T_c and T^{ch}) and elastic (between T^{ch} and T^{th}) hadronic rescatterings. Thus lower value of T^{th} with respect to T^{ch} would indicate on separate chemical and thermal freeze-out for given hadrons species. Such simplified but fast freeze-out approach is different from the simulation of full hadron cascade evolution requiring huge computing efforts.

B. Hard component

The approach for the hard component is based on the PYQUEN jet quenching model [43] modifying the nucleon-nucleon collisions generated with PYTHIA_6.4 event generator [44]. The basic kinetic equation for partonic energy loss ΔE as a function of initial energy E and path length L has the form:

$$\Delta E(L, E) = \int_0^L dl \frac{dE(l, E)}{dl} \exp(-l/\lambda(l)), \quad (4)$$

where l is the current transverse coordinate of a parton, dE/dl is the energy loss per unit length, $\lambda = 1/(\sigma\rho)$ is the in-medium mean free path, $\rho \propto T^3$ is the medium density at the temperature T , σ is the integral cross section for the parton interaction in the medium.

The radiative energy loss of massless quark is computed within BDMPS model [45–47] as

$$\frac{dE^{\text{rad}}}{dl} = \frac{2\alpha_s \mu_D^2 C_R}{\pi L} \int_{\mu_D^2 \lambda_g}^E d\omega \left[1 - x + \frac{x^2}{2} \right] \ln |\cos(\omega_1 \tau_1)|, \\ \omega_1 = \sqrt{i \left(1 - x + \frac{C_R}{3} x^2 \right) \bar{\kappa} \ln \frac{16}{\bar{\kappa}}}, \quad \bar{\kappa} = \frac{\mu_D^2 \lambda_g}{\omega(1-x)}, \quad (5)$$

where $\tau_1 = L/(2\lambda_g)$, $x = \omega/E$ is the fraction of the quark energy carried away by the radiated gluon, α_s is the QCD running coupling constant for N_f active quark flavors, $C_R = 4/3$ is the quark color factor, and μ_D is the Debye screening mass. The simple generalization of the formula (5) for a heavy quark of mass m_q is based on the “dead-cone” approximation [48]:

$$\frac{dE^{\text{rad}}}{dl} \Big|_{m_q \neq 0} = \frac{1}{(1 + (\beta\omega)^{3/2})^2} \frac{dE^{\text{rad}}}{dl} \Big|_{m_q=0}, \quad (6)$$

$$\beta = \left(\frac{\lambda}{\mu_D^2}\right)^{1/3} \left(\frac{m_q}{E}\right)^{4/3}.$$

The collisional energy loss due to elastic scatterings is calculated in the high-momentum transfer limit [49–51]:

$$\frac{dE^{\text{col}}}{dl} = \frac{1}{4T\lambda\sigma} \int_{\mu_D^2}^{t_{\text{max}}} dt \frac{d\sigma}{dt} t, \quad (7)$$

where the dominant contribution to the differential scattering cross section is

$$\frac{d\sigma}{dt} \cong C \frac{2\pi\alpha_s^2(t)}{t^2} \frac{E^2}{E^2 - m_q^2} \quad (8)$$

for the scattering of a hard quark with energy E and mass m_q off the “thermal” parton with energy $m_0 \sim 3T \ll E$, $C = 1$ and $4/9$ for qg and qq scatterings respectively. The integrated cross section σ is regularized by the Debye screening mass squared $\mu_D^2(T) \simeq 4\pi\alpha_s T^2(1 + N_f/6)$. The maximum momentum transfer is $t_{\text{max}} = [s - (m_p + m_0)^2][s - (m_p - m_0)^2]/s$ where $s = 2m_0E + m_0^2 + m_p^2$.

Note that a number of more recent and sophisticated developments in partonic energy loss calculations (for massless partons as well as for heavy quarks) are available in the literature. For example, our simplification is that the collisional energy loss due to elastic scatterings with low momentum transfer (resulting mainly from the interactions with quark-gluon plasma collective modes or color background fields) is not taken into account. In principle, in the majority of estimations, latter process does not contribute much to the total collisional loss in comparison with the high-momentum scattering, and in numerical computations it can be effectively “absorbed” by means of redefinition of minimum momentum transfer used to regularize the integral elastic cross section. Anyway, the treatment of radiative and collisional energy loss within HYDJET++ is used in current study to illustrate the influence of non-thermal component on charmed meson production features at the LHC, but it should not affect our main issues related to the thermal component.

The medium where partonic rescattering occurs is treated as a boost-invariant longitudinally expanding perfect quark-gluon fluid, and the partons as being produced on a hyper-surface of equal proper times τ [52]. The strength of partonic energy loss in PYQUEN is

determined mainly by the initial maximal temperature T_0^{max} of hot fireball in central PbPb collisions, which is achieved in the center of nuclear overlapping area at mid-rapidity. The transverse energy density in each point inside the nuclear overlapping zone is supposed to be proportional to the impact-parameter dependent product of two nuclear thickness functions T_A in this point.

Monte-Carlo simulation procedure in PYQUEN includes generation of the initial parton spectra with PYTHIA and production vertexes at given impact parameter, rescattering-by-rescattering simulation of the parton path in a dense zone, radiative and collisional energy loss per rescattering, final hadronization with the Lund string model for hard partons and in-medium emitted gluons. The PYQUEN multi-jet state is generated according to the binomial distribution, and then included in the hard component of HYDJET++ event. The mean number of jets (including heavy quark pairs) produced in AA events at a given impact parameter b is computed as

$$\overline{N_{\text{AA}}^{\text{jet}}}(b, \sqrt{s}, p_T^{\text{min}}) = \int_{p_T^{\text{min}}} dp_T^2 \int dy \frac{d\sigma_{\text{NN}}^{\text{hard}}(p_T, \sqrt{s})}{dp_T^2 dy}$$

$$\int_0^{2\pi} d\psi \int_0^\infty r dr T_A(r_1) T_A(r_2) S(r_1, r_2, p_T, y), \quad (9)$$

where $\sigma_{\text{NN}}^{\text{in}}(\sqrt{s})$ and $d\sigma_{\text{NN}}^{\text{hard}}(p_T, \sqrt{s})/dp_T^2 dy$, calculated with PYTHIA, are the total inelastic non-diffractive NN cross section and the differential cross section of the hard process in NN collisions with the minimum transverse momentum transfer p_T^{min} respectively; $r_{1,2}$ are the transverse distances between the centres of colliding nuclei and the jet production vertex. The partons produced in (semi)hard processes with the momentum transfer lower than p_T^{min} , are considered as being “thermalized”. So, their hadronization products are included “automatically” in the soft component of the event. In fact, the relative contribution of hard component into the total multiplicity is controlled by the parameter p_T^{min} . Note that some kind of transition between thermal and non-thermal components may come from a partial thermalization of hard component due to medium-induced partonic rescattering and energy loss. The factor $S \leq 1$ in (9) takes into account the effect of nuclear shadowing on parton distribution functions. It is computed using the impact parameter dependent parametrization [53] obtained in the framework of Glauber-Gribov theory.

C. Charmed mesons at RHIC

The input parameters of HYDJET++ for soft and hard components have been tuned from fitting to heavy ion data on various observables for inclusive hadrons at RHIC [32] and LHC [33].

Previously it was shown in [54] that if J/ψ -mesons are produced in HYDJET++ at the same freeze-out param-

eters as for inclusive (light) hadrons, then simulated p_T - and y -spectra in central AuAu collisions at RHIC energy $\sqrt{s_{NN}} = 200$ GeV are much wider than ones measured by PHENIX Collaboration [55]. However the assumption that the thermal freeze-out for J/ψ -mesons happens at the same temperature as chemical freeze-out with reduced radial and longitudinal collective velocities allows HYDJET++ to match the data. Note that the early thermal freeze-out of J/ψ -mesons was already suggested some years ago to describe SPS PbPb data at beam energy 158 GeV/nucleon [56]. One may argue that this is due to the higher mass and lower interaction cross section of the charmed mesons. Recently we also have checked [57] that p_T -spectrum of D -mesons measured by STAR Collaboration [58] in central AuAu collisions at $\sqrt{s_{NN}} = 200$ GeV is reproduced by HYDJET++ simulation with the same freeze-out parameters as for J/ψ -mesons, but not for inclusive hadrons. It means that D -mesons like J/ψ -mesons are not in a kinetic equilibrium with the created medium at RHIC. Then let us get a look at the LHC situation.

III. J/ψ -MESON PRODUCTION IN LEAD-LEAD COLLISIONS AT $\sqrt{s_{NN}} = 2.76$ TEV

As it was already mentioned in previous section, the input parameters of HYDJET++ have been tuned from fitting to PbPb data at $\sqrt{s_{NN}} = 2.76$ TeV for inclusive hadrons [33]. The most important parameters for our current consideration are the chemical and thermal freeze-out temperatures, $T_{ch} = 165$ MeV and $T_{th} = 105$ MeV, maximal longitudinal and transverse flow rapidities, $Y_L^{max} = 4.5$ and $Y_T^{max} = 1.265$, minimal transverse momentum transfer of initial hard scatterings $p_T^{min} = 8.2$ GeV/ c , and initial maximal temperature of quark-gluon fluid $T_0^{max} = 1$ GeV. PYTHIA_6.4 tune Pro-Q20 has been used to simulate an initial partonic state of the hard component. It reproduces the LHC data on inclusive hadron momentum spectra in pp collisions with the 10–15% accuracy in the full measured p_T -range [59].

Figure 1 shows the comparison of HYDJET++ simulations with the ALICE data [14] for p_T -spectrum of inclusive J/ψ -mesons in 20% of most central PbPb collisions at $\sqrt{s_{NN}} = 2.76$ TeV with two sets of input parameters: 1) as for inclusive hadrons (listed above), and 2) for early thermal freeze-out ($T_{ch} = T_{th} = 165$ MeV, $Y_L^{max} = 2.3$, $Y_T^{max} = 0.6$, $p_T^{min} = 3.0$ GeV/ c). The fugacity value $\gamma_c = 11.5$ was fixed from absolute J/ψ yields. One can see that the situation is similar to RHIC: simulated spectra match the data (up to $p_T \sim 3$ GeV/ c) only assuming early thermal freeze-out, which happens presumably at the phase of chemical freeze-out (with reduced collective velocities, and enhanced contribution of non-thermal component). The discrepancy at high p_T may indicate on the necessity to tune used version of PYTHIA specifically for charmonium production. However, since HYDJET++ does not include modeling of final state effects

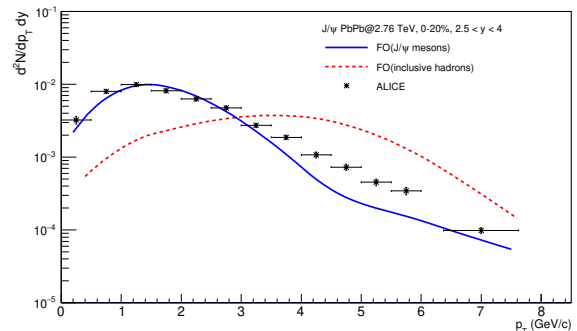


FIG. 1: Transverse momentum spectrum of inclusive J/ψ -mesons for rapidity $2.5 < y < 4$ in 20% of most central PbPb collisions at $\sqrt{s_{NN}} = 2.76$ TeV. The points denote ALICE data [14], histograms represent simulated HYDJET++ events (red dashed – freeze-out parameters as for inclusive hadrons, blue solid – early thermal freeze-out).

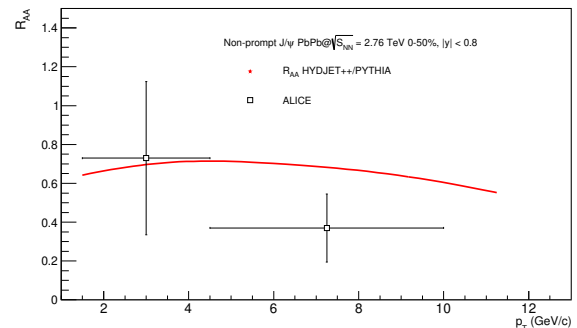


FIG. 2: Nuclear modification factor $R_{AA}(p_T)$ of non-prompt J/ψ -mesons for rapidity $|y| < 0.8$ in 50% of most central PbPb collisions at $\sqrt{s_{NN}} = 2.76$ TeV. The open squares denote ALICE data [12], the histogram represents simulated HYDJET++ events.

for quarkonia (such as a melting of primordial quarkonia in hot matter or a dissociation by comovers), it cannot pretend to reproduce the data at high transverse momenta for prompt (and so for inclusive) J/ψ mesons. On the other hand, the production of non-prompt J/ψ 's from B-meson decays is of particular interest due to a manifestation of medium-induced bottom quark energy loss in this channel, and may be analyzed within our model. The high- p_T particle production in heavy ion collisions is characterized by the nuclear modification factor R_{AA} , which is defined as a ratio of particle yields in AA and pp collisions normalized on the mean number of binary nucleon-nucleon sub-collisions $\langle N_{coll} \rangle$ for given event centrality class (calculated within HYDJET++):

$$R_{AA}(p_T) = \frac{d^2 N^{AA}/dy dp_T}{\langle N_{coll} \rangle d^2 N^{pp}/dy dp_T}. \quad (10)$$

In the absence of nuclear effects (in initial or final states) at high p_T , it should be $R_{AA} = 1$. The same version of

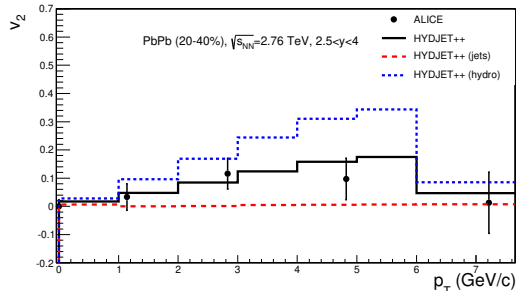


FIG. 3: Elliptic flow coefficient $v_2(p_T)$ of inclusive J/ψ -mesons for rapidity $2.5 < y < 4$ in the 20–40% centrality class of PbPb collisions at $\sqrt{s_{NN}} = 2.76$ TeV. The points denote ALICE data [9], histograms represent simulated HYDJET++ events (blue dotted – soft component, red dashed – hard component, black solid – both components).

PYTHIA_6.4 (tune ProQ20) was used to construct the pp reference for simulated events. Figure 2 shows the nuclear modification factor R_{AA} for non-prompt J/ψ -mesons as a function of p_T in 50% of most central PbPb collisions. Good model description of the ALICE data [12] is achieved up to $p_T = 4.5$ GeV/c (the first p_T bin). Some discrepancy at higher transverse momenta (the second p_T bin) may indicate again on the necessity to tune used version of PYTHIA specifically for the process under consideration. Note that the construction of pp reference for the data [12] was based on phenomenological \sqrt{s} -interpolation of the inclusive J/ψ meson production cross section and p_T distribution [60] with subsequent interpolation of prompt and non-prompt J/ψ fractions.

In addition, we found that the p_T -dependence of the elliptic flow coefficient v_2 measured by ALICE for inclusive J/ψ 's [9] is reproduced by HYDJET++ simulation in the case of early freeze-out (figure 3). An important role of non-thermal component at high p_T is clearly seen.

Thus we conclude that the significant part of J/ψ -mesons (up to $p_T \sim 3$ GeV) produced in PbPb collisions at the LHC is thermalized, but without being in kinetic equilibrium with the medium (similar to the RHIC case).

IV. D-MESON PRODUCTION IN LEAD-LEAD COLLISIONS AT $\sqrt{s_{NN}} = 2.76$ TEV

At first, we simulated D -meson production with the same freeze-out parameters as for inclusive hadrons. The fugacity value $\gamma_c = 11.5$ was fixed from J/ψ yield. Figure 4 shows the comparison of HYDJET++ simulations with the ALICE data [7] for p_T -spectra of D^\pm , $D^{*\pm}$ and D^0 mesons in 20% of most central PbPb collisions at $\sqrt{s_{NN}} = 2.76$ TeV. The simulated results are close to the data within the experimental uncertainties. Thus in contrast to RHIC, thermal freeze-out of D -mesons at the LHC happens simultaneously with thermal freeze-out of light hadrons.

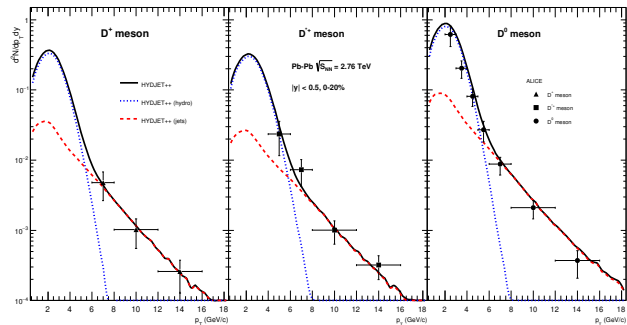


FIG. 4: Transverse momentum spectra of D^\pm (left panel), $D^{*\pm}$ (middle panel) and D^0 (right panel) for rapidity $|y| < 0.5$ in 20% of most central PbPb collisions at $\sqrt{s_{NN}} = 2.76$ TeV. The points denote ALICE data [7], histograms represent simulated HYDJET++ events (blue dotted – soft component, red dashed – hard component, black solid – both components).

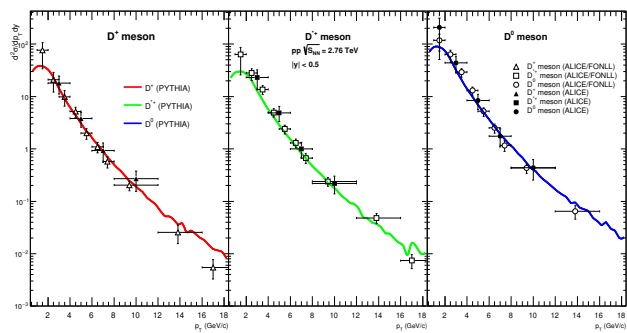


FIG. 5: Transverse momentum spectra of D^\pm (left panel), $D^{*\pm}$ (middle panel) and D^0 (right panel) for rapidity $|y| < 0.5$ in pp collisions at $\sqrt{s_{NN}} = 2.76$ TeV. The closed and open points denote ALICE data [66] and FONLL-based extrapolation of pp data from $\sqrt{s} = 7$ TeV respectively, histograms represent simulated PYTHIA_6.4 events.

To estimate the uncertainties related to choice of pp reference needed for the construction of nuclear modification factor R_{AA} (10) for D -mesons, we compare the predictions obtained from PYTHIA_6.4 (tune ProQ20) and from FONLL-based extrapolation of pp data from $\sqrt{s} = 7$ TeV. The latter procedure was utilized by ALICE Collaboration in [7]. It includes determination of the reference pp cross sections applying \sqrt{s} -scaling [61] to the cross sections measured at $\sqrt{s} = 7$ TeV [62], and obtaining the scaling factor for each D -meson species as the ratio of the cross sections from FONLL pQCD calculations [63–65] at 2.76 and 7 TeV. We have found that D -meson p_T -spectra at $\sqrt{s} = 2.76$ TeV obtained with two pp references are similar, and close to the experimental data [66] (figure 5). Note since no J/ψ -meson differential pp measurements at $\sqrt{s} = 2.76$ are currently available for the kinematic range under consideration, the construction of R_{AA} for non-prompt J/ψ -mesons in the

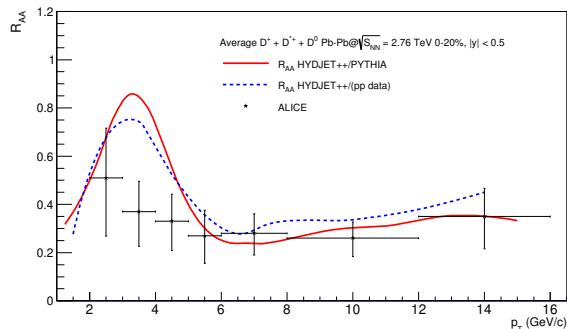


FIG. 6: Average of the three D -meson species nuclear modification factor $R_{AA}(p_T)$ for rapidity $|y| < 0.5$ in 20% of most central PbPb collisions at $\sqrt{s_{NN}} = 2.76$ TeV. The points denote ALICE data [7], histograms represent simulated HYDJET++ events for two pp references (blue dashed – extrapolated pp data, red solid – PYTHIA).

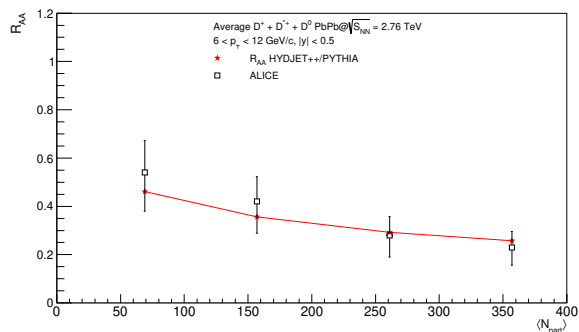


FIG. 7: Centrality dependence of average of the three D -meson species nuclear modification factor R_{AA} for rapidity $|y| < 0.5$ and $6 < p_T < 12$ GeV/c in PbPb collisions at $\sqrt{s_{NN}} = 2.76$ TeV. The open squares denote ALICE data [7], asterisks represent simulated HYDJET++ events. The line is drawn to guide the eye.

model was based on the PYTHIA simulations only (see previous section).

The p_T -dependence of average of the three D -meson species nuclear modification factor R_{AA} is presented for both pp references on figure 6. The simulated results are closed to the data up to highest $p_T = 16$ GeV. The measured centrality dependence of nuclear modification factor for high- p_T D -mesons [7] is described well by HYDJET++ simulations. This is demonstrated in figure 7, where the events are divided by four centrality classes (0–10%, 10–20%, 20–40% and 40–60%), and characterized by the average number of participating nucleons $\langle N_{part} \rangle$. In this case, PYTHIA pp reference for simulated events was used.

Finally, HYDJET++ is able to reproduce the ALICE data [8, 11] on p_T -dependence of the elliptic flow coefficient v_2 (figures 8,9).

Therefore we conclude that the significant part of D -

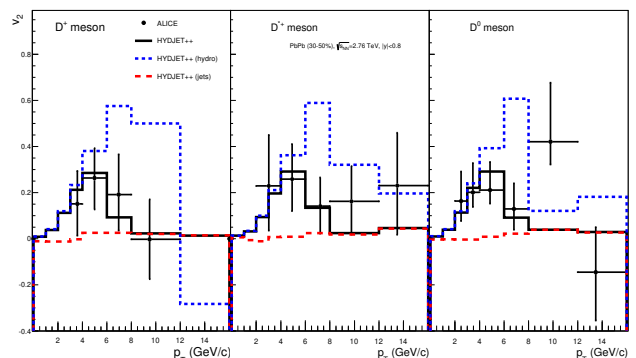


FIG. 8: Elliptic flow coefficient $v_2(p_T)$ of D^\pm (left panel), $D^{*\pm}$ (middle panel) and D^0 (right panel) mesons at rapidity $|y| < 0.8$ in the 30–50% centrality class of PbPb collisions at $\sqrt{s_{NN}} = 2.76$ TeV. The points denote ALICE data [8], histograms represent simulated HYDJET++ events (blue dotted – soft component, red dashed – hard component, black solid – both components).

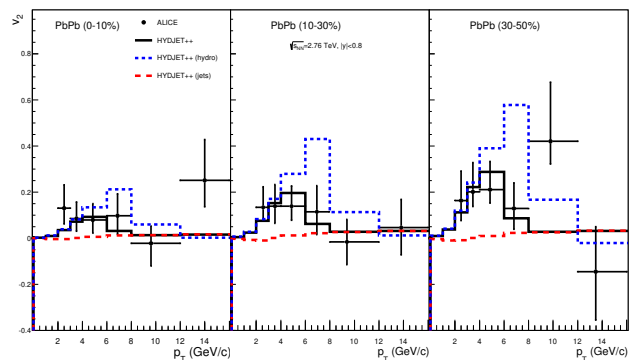


FIG. 9: Elliptic flow coefficient $v_2(p_T)$ of D^0 -mesons at rapidity $|y| < 0.8$ in the 0–10% (left panel), 10–30% (middle panel) and 30–50% (right panel) centrality classes of PbPb collisions at $\sqrt{s_{NN}} = 2.76$ TeV. The points denote ALICE data [11], histograms represent simulated HYDJET++ events (blue dotted – soft component, red dashed – hard component, black solid – both components).

mesons (up to $p_T \sim 4$ GeV/c) produced in PbPb collisions at the LHC seems to be in a kinetic equilibrium with the medium. This is quite different from the RHIC situation. The possible reason for this may be that D -meson interaction cross section at LHC energy becomes comparable with the interaction cross section of light hadrons, but J/ψ -meson interaction cross section remains much smaller. The momentum and centrality dependencies of nuclear modification factors for D^\pm , $D^{*\pm}$ and D^0 mesons at high- p_T are reproduced by HYDJET++ modeling.

V. SUMMARY

The phenomenological analysis of charmed meson production in lead-lead collisions at the center-of-mass energy 2.76 TeV per nucleon pair has been done within the two-component HYDJET++ model including thermal and non-thermal production mechanisms. Momentum spectra and elliptic flow of D and J/ψ mesons are reproduced by the model assuming that thermal freeze-out of D -mesons happens simultaneously with thermal freeze-out of light hadrons, while thermal freeze-out of J/ψ -mesons happens appreciably before, presumably at the phase of chemical freeze-out (with reduced radial and longitudinal collective velocities). Thus the significant part of D -mesons (up to transverse momenta $p_T \sim 4$ GeV/c), unlike J/ψ mesons, seems to be in a kinetic equilibrium with the created in PbPb collisions hot hadronic matter. It may indicate that D -meson interaction cross section at the LHC becomes comparable with the interaction cross section of light hadrons, but J/ψ -meson in-

teraction cross section remains significantly smaller.

Non-thermal charm production mechanism is important at high transverse momenta. A tolerable agreement of the simulated results with the data for D and non-prompt J/ψ meson nuclear modification factors testifies in favor of successful treatment of hard component within the framework of the HYDJET++ model.

VI. ACKNOWLEDGMENTS

Discussions with J. Bielcik, L.V. Bravina, A.I. Demianov, V.L. Korotkikh, L.V. Malinina, A.M. Snigirev, E.E. Zabrodin and S.V. Petrushanko are gratefully acknowledged. We thank our colleagues from ALICE and CMS collaborations for fruitful cooperation. This work was supported by the Russian Science Foundation under Grant No. 14-12-00110 in a part of computer simulation of p_T -spectrum and elliptic flow of D and J/ψ mesons in lead-lead collisions.

References

- [1] I. Arsene, *et al.* (BRAHMS Collaboration), Nucl. Phys. A **757**, 1 (2005).
- [2] B.B. Back, *et al.* (PHOBOS Collaboration), Nucl. Phys. A **757**, 28 (2005).
- [3] J. Adams, *et al.* (STAR Collaboration), Nucl. Phys. A **757**, 102 (2005).
- [4] K. Adcox, *et al.* (PHENIX Collaboration), Nucl. Phys. A **757**, 184 (2005).
- [5] N. Armesto and E. Scapparini, Eur. Phys. J. P **131**, 52 (2016).
- [6] B. Abelev *et al.* (ALICE Collaboration), Phys. Rev. Lett. **109**, 072301 (2012).
- [7] B. Abelev *et al.* (ALICE Collaboration), JHEP **1209**, 112 (2012).
- [8] B. Abelev *et al.* (ALICE Collaboration), Phys. Rev. Lett. **111**, 102301 (2013).
- [9] E. Abbas *et al.* (ALICE Collaboration), Phys. Rev. Lett. **111**, 162301 (2013).
- [10] B. Abelev *et al.* (ALICE Collaboration), Phys. Lett. B **734**, 314 (2013).
- [11] B. Abelev *et al.* (ALICE Collaboration), Phys. Rev. C **90**, 034904 (2014).
- [12] J. Adam *et al.* (ALICE Collaboration), JHEP **1507**, 051 (2015).
- [13] J. Adam *et al.* (ALICE Collaboration), JHEP **1511**, 205 (2015).
- [14] J. Adam *et al.* (ALICE Collaboration), arXiv:1506.08804, (2015).
- [15] J. Adam *et al.* (ALICE Collaboration), JHEP **1603**, 081 (2016).
- [16] J. Adam *et al.* (ALICE Collaboration), JHEP **1603**, 082 (2016).
- [17] J. Adam *et al.* (ALICE Collaboration), arXiv:1509.08802, (2015).
- [18] G. Aad, *et al.* (ATLAS Collaboration), Phys. Lett. B **697**, 294 (2011).
- [19] S. Chatrchyan, *et al.* (CMS Collaboration), JHEP **1505**, 063 (2015).
- [20] V. Khachatryan, *et al.* (CMS Collaboration), Phys. Rev. Lett. **113**, 262301 (2014).
- [21] A. Andronic, P. Braun-Munzinger, K. Redlich, and J. Stachel, J. Phys. G **38**, 124081 (2011).
- [22] J. Uphoff, O. Fochler, Z. Xu, and C. Greiner, Phys. Lett. B **717**, 430 (2012).
- [23] X. Zhao, A. Emerick, and R. Rapp, Nucl. Phys. A **904-905**, 611 (2013).
- [24] M. He, R. J. Fries, and R. Rapp, Nucl. Phys. A **910-911**, 409 (2013).
- [25] M. Nahrgang, J. Aichelin, P. B. Gossiaux, and K. Werner, Phys. Rev. C **89**, 014905 (2014).
- [26] K. Zhou, N. Xu, Z. Xu, and P. Zhuang, Phys. Rev. C **89**, 054911 (2014).
- [27] S. Cao, G. Y. Qin, and S. A. Bass, Nucl. Phys. A **931**, 569 (2014).
- [28] M. Djordjevic, M. Djordjevic, and B. Blagojevic, Phys. Lett. B **737**, 298 (2014).
- [29] A. Beraudo, A. De Pace, M. Monteno, M. Nardi, and F. Prino, Eur. Phys. J. C **75**, 121 (2015).
- [30] K. Saraswat, P. Shukla, and V. Singh, Nucl. Phys. A **943**, 83 (2015).
- [31] E. L. Bratkovskaya, T. Song, H. Berrehrh, D. Cabrera, J. M. Torres-Rincon, L. Tolos, and W. Cassing, J. Phys.: Conf. Series **668**, 012008 (2016).
- [32] I. P. Lokhtin, L. V. Malinina, S. V. Petrushanko, A. M. Snigirev, I. Arsene, and K. Tywoniuk, Comput. Phys. Commun. **180**, 779 (2009).
- [33] I. P. Lokhtin, A. V. Belyaev, L. V. Malinina, S. V. Petrushanko, E. P. Rogochnaya, and A. M. Snigirev, Eur. Phys. J. C **72**, 2045 (2012).
- [34] L. V. Bravina, B. H. Bruchheim Johansson, G. Kh. Eyyubova, V. L. Korotkikh, I. P. Lokhtin, L. V. Malinina, S. V. Petrushanko, A. M. Snigirev, and E. E. Zabrodin,

- Eur. Phys. J. C **74**, 2807 (2014).
- [35] L. V. Bravina, G. Kh. Eyyubova, V. L. Korotkikh, I. P. Lokhtin, S. V. Petrushanko, A. M. Snigirev, and E. E. Zabrodin, Phys. Rev. C **91**, 064907 (2015).
- [36] L. V. Bravina, E. S. Fotina, V. L. Korotkikh, I. P. Lokhtin, L. V. Malinina, E. N. Nazarova, S. V. Petrushanko, A. M. Snigirev, and E. E. Zabrodin, Eur. Phys. J. C **75**, 588 (2015).
- [37] N. S. Amelin, R. Lednicky, T. A. Pocheptsov, I. P. Lokhtin, L. V. Malinina, A. M. Snigirev, Iu. A. Karpenko, and Yu. M. Sinyukov, Phys. Rev. C **74**, 064901 (2006).
- [38] N. S. Amelin, R. Lednicky, I. P. Lokhtin, L. V. Malinina, A. M. Snigirev, Iu. A. Karpenko, Yu. M. Sinyukov, I. Arsene, and L. Bravina, Phys. Rev. C **77**, 014903 (2008).
- [39] A. Andronic, P. Braun-Munzinger, K. Redlich, and J. Stachel, Phys. Lett. B **571**, 36 (2003).
- [40] A. Andronic, P. Braun-Munzinger, K. Redlich, and J. Stachel, Nucl. Phys. A **789**, 334 (2007).
- [41] U. Wiedemann, Phys. Rev. C **57**, 266 (1998).
- [42] G. Torrieri, S. Steinke, W. Broniowski, W. Florkowski, J. Letessier, and J. Rafelski, Comput. Phys. Commun. **167**, 229 (2005).
- [43] I. P. Lokhtin and A. M. Snigirev, Eur. Phys. J. C **45**, 211 (2006).
- [44] T. Sjostrand, S. Mrenna, and P. Skands, JHEP **0605**, 026 (2006).
- [45] R. Baier, Yu. L. Dokshitzer, H. A. Mueller, S. Peigne, and D. Schiff, Nucl. Phys. B **483**, 291 (1997).
- [46] R. Baier, Yu. L. Dokshitzer, H. A. Mueller, S. Peigne, and D. Schiff, Phys. Rev. C **60**, 064902 (1999).
- [47] R. Baier, Yu. L. Dokshitzer, A.H. Mueller, and D. Schiff, Phys. Rev. C **64**, 057902 (2001).
- [48] Yu. L. Dokshitzer and D. Kharzeev, Phys. Lett. B **519**, 199 (2001).
- [49] J. D. Bjorken, Fermilab Preprint Pub-82/29-THY (1982).
- [50] E. Braaten and M. Thoma, Phys. Rev. D **44**, 1298 (1991).
- [51] I. P. Lokhtin and A. M. Snigirev, Eur. Phys. J. C **16**, 527 (2000).
- [52] J.D. Bjorken, Phys. Rev. D **27**, 140 (1983).
- [53] K. Tywoniuk, I.C. Arsene, L. Bravina, A.B. Kaidalov, and E. Zabrodin, Phys. Lett. B **657**, 170 (2007)
- [54] I. P. Lokhtin, A. V. Belyaev, L. V. Malinina, S. V. Petrushanko, A. M. Snigirev, I. Arsene, and E. E. Zabrodin, J. Phys.: Conf. Series **270**, 012060 (2010).
- [55] A. Adare *et al.* (PHENIX Collaboration), Phys. Rev. Lett. **98**, 232301 (2007).
- [56] K. A. Bugaev, M. Gazdzicki, and M. I. Gorenstein, Phys. Lett. B **523**, 255 (2001).
- [57] I. P. Lokhtin, A. V. Belyaev, G. Kh. Eyyubova, G. Poni-matkin, and E. Yu. Pronina, J. Phys.: Conf. Series **668**, 012068 (2016).
- [58] L. Adamczyk *et al.* (STAR Collaboration), Phys. Rev. Lett. **113**, 142301 (2014).
- [59] S. Chatrchyan *et al.* (CMS Collaboration), JHEP **1108**, 086 (2011).
- [60] F. Bossu, Z. Conesa del Valle, A. de Falco, M. Gagliardi, S. Grigoryan, and G. Martinez Garca, arXiv:1103.2394, (2011).
- [61] R. Averbeck, N. Bastid, Z. Conesa del Valle, P. Crochet, A. Dainese, and X. Zhang, arXiv:1107.3243, (2011).
- [62] B. Abelev *et al.* (ALICE Collaboration), JHEP **1201**, 128 (2012).
- [63] M. Cacciari, M. Greco, and P. Nason, JHEP **9805**, 007 (1998).
- [64] M. Cacciari, S. Frixione, and P. Nason, JHEP **0103**, 006 (2001).
- [65] M. Cacciari, S. Frixione, N. Houdeau, M. L. Mangano, P. Nason, and G. Ridolfi, JHEP **1210**, 137 (2012).
- [66] B. Abelev *et al.* (ALICE Collaboration), JHEP **1207**, 191 (2012).